

FINITE-AMPLITUDE BAROCLINIC INSTABILITY OF A MESOSCALE GRAVITY CURRENT IN A CHANNEL

CURTIS J. MOONEY and GORDON E. SWATERS*

*Applied Mathematics Institute, Department of Mathematical Sciences,
University of Alberta, Edmonton, Alberta, T6G 2G1, Canada*

(Received 15 February 1995; in final form 2 January 1996)

A finite amplitude theory is developed for the evolution of marginally unstable modes for a mesoscale gravity current on a sloping bottom. The theory is based on a nonquasigeostrophic, baroclinic model of the convective destabilization of gravity currents which allows for large amplitude isopycnal deflections while filtering out barotropic instabilities. Two calculations are presented. First, a purely temporal amplitude equation is derived for marginally unstable modes not located at the minimum of the marginal stability curve. These modes eventually equilibrate with a new finite amplitude periodic solution formed. Second, the evolution of a packet of marginally unstable modes located at the minimum of the marginal stability curve is presented. These two models are dramatically different due to fundamental physical differences. For marginally unstable modes not located at the minimum of the marginal stability curve, it is possible to determine the evolution of a single normal mode amplitude. For the marginally unstable mode located at the minimum of the marginal stability curve the entire gravity current forms a nonlinear critical layer leading to an infinity of coupled amplitude equations. If this system is truncated, on an *ad hoc* basis, to include only the fundamental harmonic and its accompanying mean flow, there exists a steadily-travelling solitary cold-core eddy solution.

KEY WORDS: Density-driven flows, gravity currents, frontal dynamics, baroclinic instability, non-linear instability.

1. INTRODUCTION

Mesoscale gravity currents are formed when dense water is formed or otherwise released in a shallow sea, such as a shelf region, and settles onto the bottom. If the bottom is sloping, then the combined influences of the Coriolis and buoyancy stresses may force the current to be transversely constrained and flow, in the northern hemisphere, with the direction of locally increasing bottom height to its right. Examples include the Denmark Strait overflow (Smith, 1976), Antarctic Bottom Water (Whitehead and Worthington, 1982), deep water formation in the Adriatic Sea (Zoccolotti and Salusti, 1987), and deep water replacement in the Strait of Georgia (LeBlond *et al.*, 1991). In particular, it is possible that the formation of propagating cold eddies or domes (e.g. Armi and D'Asaro, 1980; Houghton *et al.*, 1982; Mory *et al.*, 1987; Nof 1983; Swaters and Flierl, 1991; among others) may be the result of the instability of these currents.

Much of the theoretical work on the stability of benthic gravity currents is based on the study by Griffiths, Killworth and Stern (1982, hereinafter referred to as GKS). This study presented a long-wavelength perturbation analysis of the ageostrophic barotropic instability of a gravity current on a sloping bottom. (GKS also studied finite wavenumbers.) In order to focus attention on barotropic instability processes (i.e. the release of mean kinetic energy), GKS worked with a reduced-gravity single-layer theory in which the overlying fluid was infinitely deep and motionless. The instability was the result of a coupling of two free lateral streamlines and did not require, as in quasi-geostrophic theory (see Pedlosky, 1987, Section 7.14 or LeBlond and Mysak, 1978, Section 44), a zero in the cross-shelf potential vorticity gradient. While the instability was primarily barotropic, the unstable mode described by GKS necessarily had a concomitant release of mean potential energy. In general, the coupled front was found to be quite unstable when the width of the current was of the same scale as the Rossby deformation radius.

When GKS compared the predictions of their theory to laboratory simulations of the instability of a buoyant coupled front substantial differences were found. For example, the unstable modes described by GKS have asymptotically small along-front wavenumbers while the observed instabilities occurred over a range of wavenumbers including those corresponding to finite wavelengths. Another difficulty with the theory was that the observed instability had a dominant lengthscale independent of the current width in contradiction to the theoretical prediction.

A third aspect of the observations that the theory could not explain was a secondary branch of instabilities which had a dipole-like appearance. This difference was attributed to the existence of another, possibly baroclinic, unstable mode outside the range of applicability of the GKS analysis.

To address these issues, Swaters (1991) developed an 'intermediate lengthscale' theory for the baroclinic instability of mesoscale gravity currents. This model assumed that the dynamics of the overlying water column (see Figure 1) was quasi-geostrophically determined and that the gravity current, while the velocity field was geostrophically determined, was not quasi-geostrophic because deflections in the current height are on the same order of magnitude as the scale height for the gravity current. This balance represented a middle dynamical regime between a full geostrophic theory and the low wavenumber/frequency dynamics of quasi-geostrophic theory. This model was derived as a systematic asymptotic reduction of the full two-layer shallow-water equations for a rotating fluid on a sloping bottom and has been used to model aspects of the propagation of cold domes (Swaters and Flierl, 1991) as well as the instability calculation of Swaters (1991).

The instability mechanism modelled by Swaters is the release of the available gravitational potential energy associated with a pool of relatively dense water sitting directly on a sloping bottom surrounded by relatively lighter water. As such, this instability mechanism is phenomenologically completely different than the shear based instability associated with a buoyancy-driven current containing lighter water sitting on top of finite lower layer (e.g. Paldor and Killworth, 1987).

The Swaters' theory describes a purely baroclinic instability in that it filters out the shear based instability and exclusively models the convective destabilization of a

mesoscale gravity current on a sloping bottom. In addition, the Swaters model does not require a zero in the transverse potential vorticity gradient for instability. By allowing for finite-amplitude deformations in the current height, the Swaters' theory can describe the instability of gravity currents with isopycnals which intersect the bottom.

The intrinsically baroclinic instability of the Swaters' model differs from the non-baroclinic instability identified by GKS associated with the coupling of the two fronts in a mesoscale gravity current (for a discussion comparing these two models see Swaters, 1991). Numerical simulations based on the primitive equations (Kawase, 1994, personal communication) suggest that the convective instability mechanism is two orders of magnitude more important than any other instability mechanism for mesoscale gravity currents.

The most unstable mode in the Swaters (1991) calculation was consistent with available observations of propagating cold domes. Moreover, the theory was able to predict the onset of the curious dipole-like branch of instabilities observed in the experiments of GKS.

Notwithstanding the success of the linear instability theory, if this model is to describe the dynamical transition from an unstable gravity current to propagating cold domes, it is necessary to show that the exponentially growing instabilities eventually saturate with a new finite-amplitude configuration formed. The principal purpose of this paper is to develop a finite-amplitude instability theory for the Swaters (1991) model applied to a mesoscale gravity current on a sloping bottom.

The gravity current model examined here will be highly idealized and will not include isopycnals which intersect the bottom in a coupled front configuration. The mathematical difficulties associated with handling the finite-amplitude dynamics of isopycnals which intersect the bottom, while interesting (and ultimately the problem we want to solve), obscure the essential physics of the problem and are ignored here. After briefly examining the linear stability problem for the model gravity current, two finite-amplitude calculations are presented. In the first, we derive a purely temporal amplitude equation describing the equilibration of a marginally unstable mode which does not correspond to the mode located at the minimum of the marginal stability curve. In the second, we derive a wavepacket amplitude equation for the mode located at the minimum of the marginal stability curve, assuming it is slightly supercritical.

These two models are dramatically different due to the mathematical properties of the individual leading order linear instability problems. In the first problem, the marginally unstable mode is dispersive so that higher order harmonics do not directly produce secularities in the asymptotic analysis developed here. Our derivation of the temporal amplitude equation for this problem is straight-forward and closely follows the classical work of Pedlosky (1970) modified for our governing equations.

However, the leading order solution for the marginally unstable mode located at the minimum of the marginal stability curve has the property that the two layers are uncoupled and the Doppler-shifted frequency in the gravity current is zero. This is identical to the situation that occurs in the Phillip's model of quasi-geostrophic (QG) baroclinic instability for a marginally unstable flow (e.g.,

Pedlosky, 1982a). This fact has important physical and theoretical implications. As pointed out by Pedlosky (1982b) and further commented on by Warn and Gauthier (1989), in the context of the Phillip's model of baroclinic instability, this will imply that the entire lower layer forms a critical layer in which advection of the perturbation field by itself cannot be neglected even at lowest order, i.e., the evolution of the perturbation flow in the lower layer is nonlinear at leading order (see, e.g., Benny and Bergeron, 1969). A similar situation occurs in the theory developed here for a marginally unstable mesoscale gravity current, i.e., the gravity current, to leading order, forms a critical layer.

From the viewpoint of examining the spectrum of the evolving perturbation flow for the marginally unstable mode located at the minimum of the marginal stability curve, the above remarks necessarily imply that a single mode cannot be generated in isolation in the gravity current layer but rather an infinity of modes are generated (see, e.g., the early incorrect QG instability theory in Pedlosky, 1972, and the later corrected theory in Pedlosky, 1982a). We show that, within the context of a wave packet analysis of a marginally unstable gravity current, the evolution of the perturbation field is governed by a denumerable infinity of coupled wavepacket equations. Thus, the finite-amplitude development of the marginally unstable mode located at the minimum of the marginal stability curve is rather different from other modes on the marginal stability curve which do not necessarily lead to a rapid development of an infinite number of leading order modes in the spectrum of the perturbation field.

Alternatively, from a mathematical viewpoint of the asymptotics involved, the distinguished limit associated with the marginal stability mode located at the minimum of the marginal stability curve has the leading order equation for the gravity current decoupled from the upper layer and nondispersive in character. As is well known in the theory of hyperbolic partial differential equations, this means that all higher harmonics will necessarily give rise to secularities in the first order perturbation equations in the underlying asymptotic expansion. An infinite number of coupled wave packet evolution equations is therefore necessary in order to construct a uniformly valid asymptotic theory over the time scale associated with the nonlinear development.

The analysis of these amplitude equations is complicated. In the limit in which the wave amplitudes are only a function of time, it is formally possible to exactly solve for the perturbation field using a method developed by Warn and Gauthier (1989). If spatial variations are retained in the wave amplitude equations, there is no known method of exact solution. Nevertheless, we show that if one retains, on a purely *ad hoc* basis, only the principal harmonic and its accompanying mean flow, there exists a steadily-travelling solitary cold-core eddy solution to the envelope equations. We also numerically investigate the temporal problem associated with higher order truncations in order to qualitatively describe the bounded, periodic solutions that can occur.

The paper is set out as follows. In Section 2, the model is derived, and in Section 3 the results of linear theory are briefly summarized. In Section 4, weakly nonlinear theory is applied to an unstable mode which is not located at the bottom of the marginal stability curve, and in Section 5, the amplitude equations are derived for

the mode which is located at the bottom of the marginal stability curve. The results are summarized and conclusions drawn in Section 6.

2. FORMULATION OF THE MODEL

The derivation of the equations has been described elsewhere (Swaters and Flierl, 1991; Swaters, 1991; Swaters, 1993) and so our presentation will be relatively brief. The physical geometry corresponds to an f -plane two-layer fluid in a channel of width L with a linearly sloping bottom (see Fig. 1). The right-handed along-channel and across-channel coordinates are x and y , respectively, and t is time. Alphabetical subscripts, except where indicated, represent partial differentiation, and $\nabla = (\partial_x, \partial_y)$.

If the geostrophic pressure in the upper layer is denoted by $\eta(x, y, t)$ and the lower layer current height (relative to the sloping bottom) is denoted as $h(x, y, t)$, then the non-dimensional governing equations can be written in the form

$$(\nabla^2 \partial_t - \partial_x) \eta - h_x + J(\eta, \nabla^2 \eta) = 0, \tag{2.1}$$

$$h_t + h_x + J(\eta, h) = 0, \tag{2.2}$$

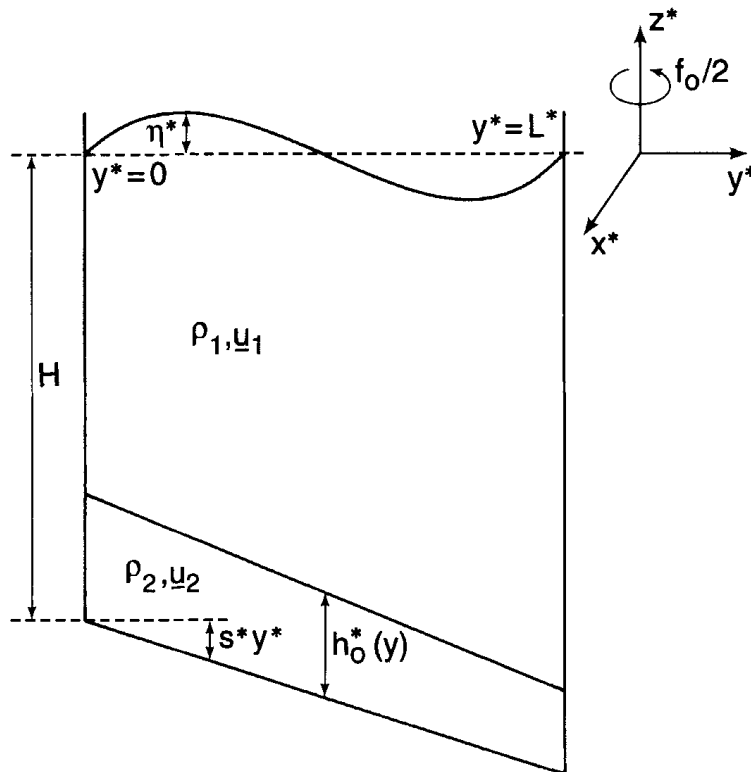


Figure 1 Geometry of the channel two-layer model.

where $J(A, B) \equiv A_x B_y - A_y B_x$. Given η and h , the velocity in the upper and lower layers and the geostrophic pressure are given by, respectively,

$$\mathbf{u}_1 = \hat{\mathbf{e}}_3 \times \nabla \eta, \quad (2.3)$$

$$\mathbf{u}_2 = \hat{\mathbf{e}}_1 + \hat{\mathbf{e}}_3 \times \nabla(\eta + h), \quad (2.4)$$

$$p = -y + \eta + h. \quad (2.5)$$

With respect to boundary conditions, if the location of the channel walls are denoted by $y=0$ and L , respectively, then the no normal flow conditions are simply $h_x = \eta_x = 0$ on $y=0$ and L , respectively.

The non-dimensionalized variables are related to the dimensional (asterisked) variables via the relations

$$\left. \begin{aligned} (x^*, y^*) &= L^*(x, y), & t^* &= fL^*(g' s^*)^{-1} t, & h^* &= sHh, \\ \mathbf{u}_1^* &= s f L^* \mathbf{u}_1, & \eta^* &= s (fL^*)^2 g'^{-1} \eta, & \mathbf{u}_2^* &= s g' H (fL^*)^{-1} \mathbf{u}_2, \\ p^* &= s \rho_2 g' H p, \end{aligned} \right\} \quad (2.6)$$

where the horizontal length scale is the internal deformation radius $L^* = \sqrt{g'H/f}$, g' is the reduced gravity and $s = s^* L^*/H$ is a scaled bottom slope parameter where s^* is the unscaled bottom slope parameter and H is the mean depth of the upper layer.

We briefly remark here that the equations (2.1) and (2.2) correspond to an asymptotic limit (i.e., $0 < s \ll 1$) of the full two-layer shallow water equations in which the evolution of the upper layer is quasi-geostrophic but the lower layer, while geostrophic, is not quasi-geostrophic and allows for large-amplitude thickness variations, i.e., allows for frontal configurations in which the lower layer height can intersect the bottom. We also remark that while the geostrophic assumption in the cross-frontal direction in some density-driven flows is inappropriate, the observations of meso-scale gravity currents which have motivated this study support this approximation (e.g. Stacey *et al.*, 1987, 1988, 1991; LeBlond *et al.*, 1991; Karsten *et al.*, 1995). From the point of view of interpreting (2.1) and (2.2) in the context of potential vorticity dynamics, we note that (2.1) + (2.2) is the $O(s)$ potential vorticity equation associated with the upper layer and (2.2) is the $O(1)$ potential vorticity equation associated with the gravity current.

Finally, we point out that (2.1) and (2.2) admits the steady parallel shear flow solution

$$\eta = \eta_0(y) = - \int_0^y \dot{U}_0(\zeta) d\zeta, \quad h = h_0(y), \quad (2.7,8)$$

where $h_0(y)$ is assumed to be everywhere nonnegative on physical grounds. This is the general class of steady solutions that we focus on for the remainder of this paper.

3. LINEAR STABILITY PROBLEM

In Swaters (1991), a comprehensive linear stability analysis was performed for a coupled density front on a semi-infinite sloping continental shelf with only one boundary. Since the details of this study are much the same, we present only a brief outline.

In order to derive the stability equations, we introduce

$$\eta = \eta_0(y) + \eta'(x, y, t), \quad h = h_0(y) + h'(x, y, t), \quad (3.1)$$

where η' and h' are the perturbation fields and substitute into (2.1) and (2.2) using (2.7) and (2.8) to get (after dropping the primes)

$$\left. \begin{aligned} [\partial_t + U_0 \partial_x] \nabla^2 \eta - (1 + U_{0yy}) \eta_x - h_x + J(\eta, \nabla^2 \eta) &= 0, \\ [\partial_t + (U_0 + 1) \partial_x] h + h_{0y} \eta_x + J(\eta, h) &= 0. \end{aligned} \right\} \quad (3.2)$$

These are the nonlinear perturbation equations, and they will be used in the weakly nonlinear analyses presented in the next two sections. For our purposes in this section, we drop the Jacobian terms, which are quadratic in the perturbations, to arrive at the linear stability equations

$$\left. \begin{aligned} [\partial_t + U_0 \partial_x] \nabla^2 \eta - (1 + U_{0yy}) \eta_x - h_x &= 0, \\ [\partial_t + (U_0 + 1) \partial_x] h + h_{0y} \eta_x &= 0. \end{aligned} \right\} \quad (3.3)$$

We now introduce along-front normal mode instabilities of the form

$$[\eta, h] = [\tilde{\eta}(y), \tilde{h}(y)] \exp[ik(x - ct)] + \text{c.c.}, \quad (3.4)$$

where c.c. means complex conjugate, k is the real-valued along-channel wavenumber, and c is the along-channel complex wave speed. Substituting (3.4) into (3.3) gives (after dropping the tildes)

$$\left. \begin{aligned} (c - U_0)(\eta_{yy} - k^2 \eta) + [1 + U_{0yy} + h_{0y}(c - 1 - U_0)^{-1}] \eta &= 0, \\ h &= h_{0y}(c - 1 - U_0)^{-1} \eta. \end{aligned} \right\} \quad (3.5)$$

Swaters (1991) showed that a necessary condition for instability in this model is that $h_{0y}(y) < 0$ for some value of y . In this paper, we assume that the gravity current takes the form of a simple wedge described by

$$h_0(y) = h_{\text{MAX}} - \gamma y, \quad \gamma > 0. \quad (3.6)$$

Here γ is the cross-channel rate of change of the thickness of the gravity current relative to the sloping bottom and h_{MAX} is the maximum height of the gravity current in non-dimensional units. The dimensional rate of change of the mean thickness is given by $\gamma^* = (h^*/L^*)\gamma$ and the dimensional maximum height is $h_{\text{MAX}}^* = sHh_{\text{MAX}}$; see (2.6).

We now concentrate on the ‘pure’ baroclinic problem for the remainder of this paper by setting the upper layer mean flow $U_0 = 0$. This approximation filters out any possible barotropic instability in the upper layer associated with any possible shear in the upper layer independent of the baroclinicity. After inserting (3.6) into (3.5) we find

$$\eta_{yy} - \left\{ k^2 - \frac{1}{c} + \frac{\gamma}{c(c-1)} \right\} \eta = 0, \quad h = -\frac{\gamma}{c-1} \eta, \quad (3.7)$$

with the boundary conditions

$$\eta = 0 \text{ and } h = 0 \quad \text{on } y = 0, L. \quad (3.8)$$

The solution to (3.7a), subject to (3.8), is

$$\eta = a_1 \sin(n\pi y/L) \quad \text{for } n = 1, 2, 3, \dots, \quad (3.9)$$

where a_1 is a free constant with the dispersion relation

$$c = \frac{k^2 + l^2 + 1 \pm [(k^2 + l^2 + 1)^2 - 4(k^2 + l^2)(1 + \gamma)]^{1/2}}{2(k^2 + l^2)}, \quad (3.10)$$

where $l = n\pi/L$.

For instability to occur, c must have a complex component. The boundary between instability and stability will be given, therefore, by setting the quantity in equation (3.10) under the square root sign to zero. This gives us the marginal stability curve, whose equation can be written in the form

$$\gamma_c = (K^2 - 1)^2 / 4K^2, \quad (3.11)$$

where γ_c is the critical value of γ above which the $K^2 \equiv k^2 + l^2$ mode goes unstable.

Figure 2 shows a plot of the marginal stability curve. The minimum of the marginal stability curve is located at $K = 1$ and $\gamma_c = 0$. Thus for every $\gamma_c > 0$, there exists wavenumbers which are unstable.

We can easily determine the range of along-channel wavenumbers k which are unstable for given γ from (3.10). A given (k, l) -mode is unstable if

$$(k^2 + l^2 + 1)^2 - 4(k^2 + l^2)(1 + \gamma) < 0, \quad (3.12)$$

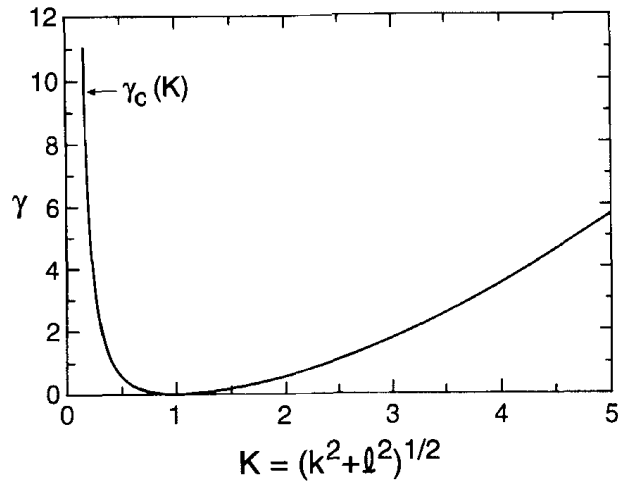


Figure 2 Marginal stability curve as determined from equation (3.11).

which can be re-arranged into

$$0 < 1 + 2\gamma - 2(\gamma + \gamma^2)^{1/2} < k^2 + l^2 < 1 + 2\gamma + 2(\gamma + \gamma^2)^{1/2}. \tag{3.13}$$

It follows that the length of the k -interval for which there is instability as a function of l does not change until

$$l = [1 + 2\gamma - 2(\gamma + \gamma^2)^{1/2}]^{1/2}, \tag{3.14}$$

after which it decreases as l increases until

$$l = [1 + 2\gamma + 2(\gamma + \gamma^2)^{1/2}]^{1/2}, \tag{3.15}$$

after which there are no unstable modes.

Furthermore, we see that $n\pi/L < 1$ for at least $n = 1$ for the $K = 1$ mode to exist. Consequently, henceforth we shall set $l = \pi/L$. Finally, we note that if L is very large than we have a useful model for continental shelf dynamics because the offshore boundary is effectively unbounded.

It is possible to see the difference between the dynamics of the $K = 1$ and $K \neq 1$ modes already at this point. If we substitute (3.6) with $\gamma = \gamma_c$ and $U_0 = 0$ into (3.3), assuming normal mode solutions of the form

$$[\eta, h] = [\hat{\eta}, \hat{h}] \sin(l y) \exp [ik(x - ct)] + \text{c.c.}, \tag{3.16}$$

we obtain the matrix system

$$\begin{bmatrix} cK^2 - 1 & -1 \\ \frac{(K^2 - 1)^2}{4K^2} & c - 1 \end{bmatrix} \begin{bmatrix} \hat{\eta} \\ \hat{h} \end{bmatrix} = \mathbf{0}.$$

For a nontrivial solution the determinant of the matrix must be zero which yields the double root $c = (K^2 + 1)/(2K^2)$. However, the null space associated with this root is only one-dimensional, i.e., $[\hat{\eta}, \hat{h}] \propto [2, K^2 - 1]$. This follows, of course, from the fact that the instability may be thought of as the coalescence of two neutral modes. The fact that \hat{h} is proportional to $\hat{\eta}$ if $K^2 \neq 1$ will allow us, as we show in Section 4, to derive a single amplitude equation for the nonlinear evolution of a marginally unstable mode not located at the minimum of the marginal stability curve. However, at the minimum of the marginal stability curve where $K^2 = 1$ we have $c = 1$ and hence $\hat{h} = 0$. Thus, the evolution of h will be determined by higher order, that is, the nonlinear terms in (3.2b). As we shall see Section 5, this will result in an infinite number of modes being required to describe h .

4. AMPLITUDE EQUATION FOR THE $K \neq 1$ MODES

In order to see how the unstable modes as determined by linear theory actually evolve in time and space we must allow the nonlinear interactions to be included in the description of the physical process. That is, we must develop a finite amplitude theory which follows the evolution of the wave when it has reached amplitudes for which the linear theory is no longer valid.

4.1. Derivation of the amplitude equation

In this section, we derive a temporal amplitude evolution equation for a weakly unstable mode which has a wavenumber modulus different than $K = 1$. In this situation, there will always be other modes with different wavenumbers which are unstable at smaller values of γ . Because of this, in this section we do not utilize a slow space variable which would follow the evolution of a wavepacket centered on the mode in question. We remark that it is straightforward to include a slow space variable for these modes in a manner which has been recently described for the Phillip's model (e.g., Tan and Liu, 1995). Also, we point out that in some sense the analysis presented in this section is somewhat artificial in that there will always be wavenumbers K for the same γ which are more unstable than the wavenumber being considered. Nevertheless, it is instructive, if not the most physically relevant, to consider a marginally unstable $K \neq 1$ mode.

To determine the proper scaling for the slow time variable, we look at the dispersion relation (3.10). From this it can be seen that if γ_c is increased to $\gamma_c + \Delta$, where Δ is a small number, the corresponding increase in the growth rate will be propor-

tional to $\Delta^{1/2}$. This means that if we let $\varepsilon^2 = \Delta$ (for convenience), then we write the following to represent a small supercriticality in γ

$$\gamma = \gamma_c + \varepsilon^2, \tag{4.1}$$

which, according to the above discussion, leads us to introduce the slow timescale and weakly nonlinear scaling

$$(\eta, h)(x, y, t) = \varepsilon(\tilde{\eta}, \tilde{h})(x, y, t, T), \quad T = \varepsilon t. \tag{4.2}$$

We note that $T \approx O(1)$, i.e., $t \approx O(\varepsilon^{-1})$ will be the timescale over which the instability evolves nonlinearly.

We take equations (3.2), which are the nonlinear perturbation equations, and (3.6), and substitute in (4.1) and (4.2), drop the tildes, set $U_0 \equiv 0$, and notice that the time derivative mapping as a result of (4.2) is $\partial_t \mapsto \partial_t + \varepsilon \partial_T$. This yields

$$\left. \begin{aligned} \nabla^2 \eta_t - \eta_x - h_x &= -\varepsilon \nabla^2 \eta_T - \varepsilon J(\eta, \nabla^2 \eta), \\ h_t + h_x - \gamma_c \eta_x &= -\varepsilon h_T + \varepsilon^2 \eta_x - \varepsilon J(\eta, h). \end{aligned} \right\} \tag{4.3}$$

The marginally unstable ansatz corresponds to assuming $0 < \varepsilon \ll 1$ and constructing an asymptotic solution to (4.3) in the form

$$\left. \begin{aligned} \eta(x, y, t, T) &= \eta^{(0)}(x, y, t, T) + \varepsilon \eta^{(1)}(x, y, t, T) + \dots, \\ h(x, y, t, T) &= h^{(0)}(x, y, t, T) + \varepsilon h^{(1)}(x, y, t, T) + \dots \end{aligned} \right\} \tag{4.4}$$

A cautionary note is required here with respect to this asymptotic expansion. We remind the reader that the governing equations (2.1) and (2.2) are themselves the result of an asymptotic expansion in the scaled slope parameter s introduced in (2.6). The asymptotic expansion we develop in this section and in Section 5 will be consistent with the derivation of (2.1) and (2.2) if $0 < s \ll \varepsilon^2 \ll \varepsilon \ll 1$. We have argued elsewhere (e.g., Swaters and Flierl, 1991) that $s \approx 0.07$ for typical flows of interest on a continental shelf implying that ε cannot be much smaller than about 0.3. It may seem unreasonable to construct an asymptotic expansion with such a large value of ε . We argue, however, that much can be learned from examining this limit and the asymptotic dynamical balances which result correctly describe the qualitative behavior of the nonlinear development of the marginally unstable modes.

The $O(1)$ problem associated with substituting (4.4) into (4.3), is given by

$$\left. \begin{aligned} \nabla^2 \eta_t^{(0)} - \eta_x^{(0)} - h_x^{(0)} &= 0, \\ h_t^{(0)} + h_x^{(0)} - \gamma_c \eta_x^{(0)} &= 0. \end{aligned} \right\} \tag{4.5}$$

The solution for the equations (4.5) will be in the form

$$\begin{aligned}\eta^{(0)} &= A(T)\sin(l y)\exp(ik\theta) + \text{c.c.}, \\ h^{(0)} &= B(T)\sin(l y)\exp(ik\theta) + \text{c.c.},\end{aligned}$$

where $\theta = x - ct$, c is a *real* phase speed, $l = \pi/L$, c.c. is complex conjugate, and A, B are the amplitude coefficients.

Substitution of (4.6) into (4.5) leads to

$$c = \frac{k^2 + l^2 + 1}{2(k^2 + l^2)}, \quad (4.7)$$

which is the dispersion relation found in Section 3 using linear theory after utilizing (3.11), and

$$B = \gamma_c A / (1 - c) = \frac{1}{2}(k^2 + l^2 - 1)A, \quad (4.8)$$

which is the equation relating the amplitude of $h^{(0)}$ to that of $\eta^{(0)}$. This will be utilized in later calculations.

The $O(\varepsilon)$ problem is given by

$$\left. \begin{aligned}\nabla^2 \eta_t^{(1)} - \eta_x^{(1)} - h_x^{(1)} &= -\nabla^2 \eta_T^{(0)} - J(\eta^{(0)}, \nabla^2 \eta^{(0)}), \\ h_t^{(1)} + h_x^{(1)} - \gamma_c \eta_x^{(1)} &= -h_T^{(0)} - J(\eta^{(0)}, h^{(0)}).\end{aligned}\right\} \quad (4.9)$$

Substituting in the solutions from the $O(1)$ problem, we find

$$\nabla^2 \eta_t^{(1)} - \eta_x^{(1)} - h_x^{(1)} = A_T (k^2 + l^2) \sin(l y) \exp(ik\theta) + \text{c.c.}, \quad (4.10)$$

$$h_t^{(1)} + h_x^{(1)} - \gamma_c \eta_x^{(1)} = -B_T \sin(l y) \exp(ik\theta) + \text{c.c.} \quad (4.11)$$

The solution to (4.10) and (4.11) may be written in the general form

$$\left. \begin{aligned}\eta^{(1)} &= E(T)\sin(l y)\exp(ik\theta) + \text{c.c.}, \\ h^{(1)} &= \phi(y, T) + F(T)\sin(l y)\exp(ik\theta) + \text{c.c.},\end{aligned}\right\} \quad (4.11)$$

where $\phi(y, T)$ is a homogeneous solution which results from nonlinear interactions in the $O(\varepsilon^2)$ problem.

Substitution of (4.12) into (4.10) and (4.11) yields, after some algebra, a relation between F and E of the form

$$F = \frac{\gamma_c E}{1 - c} + i \frac{\gamma_c A_T}{k(1 - c)^2}. \quad (4.13)$$

Using (4.13) in (4.10) and the values for c as determined by the dispersion relation (4.7), we find

$$\left. \begin{aligned} \eta^{(1)} &= 0, \\ h^{(1)} &= \phi(y, T) + i \frac{\gamma_c A_T}{k(1-c)^2} \sin(ly) \exp(ik\theta) + \text{c.c.}, \end{aligned} \right\} \quad (4.14)$$

i.e., $E \equiv 0$, that is, the homogeneous solution is absorbed, without loss of generality, into the $O(1)$ solutions. The required evolution equation for $A(T)$ is determined by examining the $O(\varepsilon^2)$ problem given by

$$\left. \begin{aligned} \nabla^2 \eta_t^{(2)} - \eta_x^{(2)} - h_x^{(2)} &= -\nabla^2 \eta_T^{(1)} - J(\eta^{(1)}, \nabla^2 \eta^{(0)}) - J(\eta^{(0)}, \nabla^2 \eta^{(1)}), \\ h_t^{(2)} + h_x^{(2)} - \gamma_c \eta_x^{(2)} &= -h_T^{(1)} + \eta_x^{(0)} - J(\eta^{(1)}, h^{(0)}) - J(\eta^{(0)}, h^{(1)}). \end{aligned} \right\} \quad (4.15)$$

Using (4.14) and (4.6) in (4.15) we find

$$\left. \begin{aligned} \nabla^2 \eta_t^{(2)} - \eta_x^{(2)} - h_x^{(2)} &= 0 \\ h_t^{(2)} + h_x^{(2)} - \gamma_c \eta_x^{(2)} &= \left[-\frac{i}{k} \left(\frac{\gamma_c A_{TT}}{(1-c)^2} \right) + ikA - ikA\phi_y \right] \sin(ly) \exp(ik\theta) + \text{c.c.} \\ &\quad - \phi_T - [2ikl(AD_T^* - A^*D_T) \sin(ly) \cos(ly)], \end{aligned} \right\} \quad (4.16)$$

where

$$D_T = i \frac{\gamma_c A_T}{k(1-c)^2}. \quad (4.17)$$

Now we apply solvability conditions to (4.16b) in order to determine the amplitude equation. Since all the terms in the left-hand side of this equation contain derivatives in either x or t , the coefficient of the inhomogeneities on the right-hand side which are independent of x and t must vanish. This leads to

$$\phi_T = -2ikl(AD_T^* - A^*D_T) \sin(ly) \cos(ly). \quad (4.18)$$

Using the expression for D_T and a trigonometric identity, this may be written as

$$\phi_T = -\frac{\gamma_c l}{(1-c)^2} (|A|^2)_T \sin(2ly), \quad (4.19)$$

Now integrating (4.19) with respect to T , we find, after applying (3.11) and the dispersion relation (4.7)

$$\phi = -lK^2 (|A|^2 - |A_0|^2) \sin(2ly), \quad (4.20)$$

where $A_0 = A(T=0)$. It is important to note that ϕ , the adjustment to the mean flow, is always strictly real.

Another point to appreciate is that the differential equation for $\phi(y, T)$ given by (4.19) does not contain any derivatives with respect to the cross-channel coordinate y . Thus, it is not possible to impose additional auxiliary boundary conditions at $y=0, L$ on ϕ as one needs to do in quasi-geostrophic theory (Pedlosky, 1970). The reason why there are no y -derivatives in (4.19) arises from the fact that the convective time derivatives in the momentum equations for the gravity current have been completely filtered out in the derivation of the governing equations (2.1) and (2.2). The additional auxiliary boundary conditions for the x -independent mean flow required in finite amplitude quasi-geostrophic baroclinic instability are derived from the local time rate of change of momentum terms which are retained in quasigeostrophic theory. Since these terms are not retained here in any form it is inappropriate to expect that ϕ should satisfy conditions which are derived from them. We note, however, that the $\sin(2ly)$ dependence in the solution for ϕ will imply that there is no net along-channel mass flux associated with the mean flow, i.e., generated by the self-interaction of the perturbation wave field to this order. This means that

$$\int_0^L \phi_y dy = 0. \quad (4.21)$$

To derive the required evolution for $A(T)$ it is convenient to first eliminate $h^{(2)}$ between (4.16a) and (4.16b) to yield

$$(\partial_t + \partial_x)(\nabla^2 \partial_t - \partial_x)\eta^{(2)} - \gamma_c \eta_{xx}^{(2)} = \left[\frac{\gamma_c A_{TT}}{(1-c)^2} - k^2 A - \frac{2\gamma_c k^2 l^2 A}{(1-c)^2} (|A|^2 - |A_0|^2 \cos(2ly)) \right] \exp(ik\theta) \sin(ly) + \text{c.c.} \quad (4.22)$$

Using another trigonometric identity we may re-write $\cos(2ly)\sin(ly)$ as $[\sin(3ly) - \sin(ly)]/2$. The only terms which produce secular growth are those terms on the right-hand side of (4.22) which are proportional to $\sin(ly)\exp(ik\theta)$ and its complex conjugate. Setting the coefficient of these terms to zero yields the desired amplitude equation

$$A_{TT} = \sigma^2 A - NA(|A|^2 - |A_0|^2), \quad (4.23)$$

where $\sigma \equiv [k^2/(k^2 + l^2)]^{1/2}$ and $N \equiv k^2 l^2$ and where we have used (3.11) and (4.7). Note that σ represents the growth rate for the unstable mode as would be determined from the linear theory. Pedlosky (1970) derived a similar evolution equation from a two-layer, rigid-lid model of quasigeostrophic baroclinic instability on a β -plane.

The method of solution for (4.23) follows Pedlosky (1987) exactly, and so we merely provide an outline. Assuming a solution to (4.23) of the form

$$A(T) = R(T)\exp[i\theta(T)], \tag{4.24}$$

leads to, after separating the real imaginary parts,

$$\left. \begin{aligned} \theta_T &= M/R^2, \\ R_{TT} - M^2/R^3 &= \sigma^2 R - NR(R^2 - R_0^2), \end{aligned} \right\} \tag{4.25}$$

where M is a constant. If we assume that the phase is constant in time, then $M = 0$ and (4.25b) becomes

$$R_{TT} = \sigma^2 R - NR(R^2 - R_0^2). \tag{4.26}$$

The constant phase for A means that at $T=0$, $dA/dT = \sigma A$, that is, the amplitude increases initially according to the growth rate specified by linear theory.

If (4.26) is multiplied by R_T and integrated, we obtain

$$\frac{1}{2}R_T^2 + V(R) = E, \tag{4.27}$$

where $V(R) = -R^2(\sigma^2 + NR_0^2) + NR^4/4$ and E is a constant. Pedlosky (1987) has shown that (4.27) may be written as

$$d\tau = \frac{d\xi}{[(1 - \xi^2)(\xi^2 - \alpha^2)]^{1/2}}, \tag{4.28}$$

where $\xi = R/R_{\max}$, $\alpha = R_{\min}/R_{\max}$ and $\tau = (NR_{\max}^2/2)^{1/2} T$ and where

$$R_{\max,\min}^2 = R_0^2 + \frac{\sigma^2}{N} \left[1 \pm \left(1 + \frac{2NR_0^2}{\sigma^2} \right)^{1/2} \right], \tag{4.29}$$

where the max and min are associated with the plus and minus signs, respectively. Integrating (4.28) leads to

$$\xi = dn(\tau - \tau_0|m), \tag{4.30}$$

where

$$\tau_0 = dn^{-1} \left(\frac{R_0}{R_{\max}} \middle| m \right). \tag{4.31}$$

Here dn is the Jacobi elliptic dnoidal function [following the notation of Milne-Thomson (1950)], $m = (1 - \alpha^2)$, and τ_0 is chosen in such a way as to ensure that

$R = R_0$ at $\tau = 0$. The period of the disturbance is given by

$$\tau_p = 2E(m), \quad (4.32)$$

where $E(m)$ is the complete Jacobi elliptic integral of the first kind.

The evolution of A follows the form of a dnoidal wave, and therefore is periodic in time. This means that after the initial exponential increase of the unstable mode the effect of the nonlinearities in the equations for A is to slow and eventually reverse the growth of the disturbance. The amplitude falls until it reaches a point where the linear growth rate becomes dominant again, and the cycle begins anew.

4.2. Description of the solutions for the dnoidal wave equation

In this subsection, we examine the amplitude function derived in the previous subsection, redimensionalize it and see what it means for the physical problem that was enunciated at the outset.

The scalings presented in Section 2, as mentioned before, suggest horizontal lengthscales of order 15 km, advective timescales of order 7 days, and a scale height for the gravity current of about 40 m. Let us consider a channel width $L = \pi$ in non-dimensional units, so that we set the cross-channel wavenumber, $l = \pi/L$, equal to 1 (this corresponds to a dimensional channel width of about 47 km).

As an example, if we set $k = 1$, then the solution (4.30) corresponds to the horizontal mode $K = \sqrt{2}$. We also let $\varepsilon = 0.1$ and the initial non-dimensional perturbation pressure amplitude $A_0 = 0.1$. With these parameters, the amplitude function $A(T)$ is found to vary with slow time as depicted in Figure 3. From this plot, it can be seen

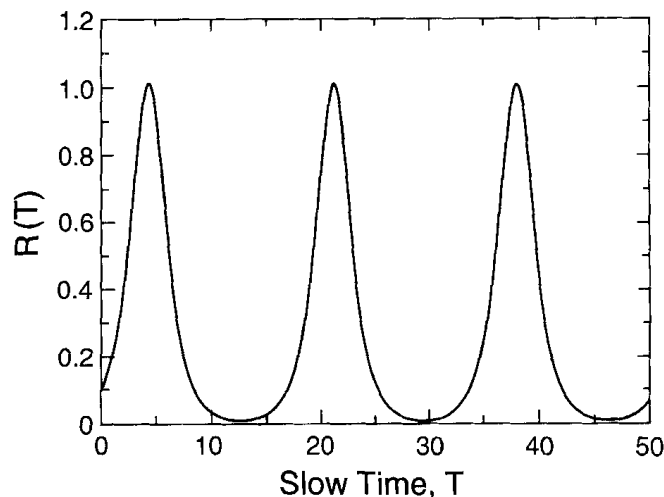


Figure 3 Plot of non-dimensional perturbation pressure amplitude $R(T)$ versus time T , where $k = l = 1.0$ (i. e. $N = 1.0$), $\varepsilon = 0.1$ and where $\eta = \varepsilon\eta_0 + O(\varepsilon^2)$.

that the oscillations at this wavenumber are such that R grows to about 10 times its initial amplitude before saturating. The period is about 20 slow time units. The ultra-long period is indicative of nothing more than the fact that the supercriticality is very small [i.e. $O(\varepsilon^2)$]. This produces a small growth rate which eventually is balanced by a similarly scaled nonlinearity. This is certainly a weakness in the model, but our main purpose has been to show that the nonlinearities will slow and reverse the linear growth rate of the disturbance. Since this is the situation, we expect that in the full nonlinear case, where the supercriticality could be much larger than $\gamma_c + \varepsilon^2$, there exists the possibility that the wave will be large enough to break up the gravity current into coherent travelling eddies or, equally likely, accelerate the instability further.

Analyses similar to what was presented above may be done for each along-channel wavenumber. To see how the key parameters change as k changes, we present the following plots. Figure 4 shows how the maximum amplitude, R_{\max} , varies with wavenumber. It can be seen that as the wavelength becomes shorter, the maximum amplitude decreases, becoming more or less constant with an 85% reduction at the high wavenumber limit. Figure 5 is a plot of the period of the disturbance as it varies with k . From this figure, we see that the period falls off as the along-channel wavenumber increases, very much like the period of the fast along-channel oscillations would be expected to change. So from the above discussion it can be concluded that as the wavenumber increases, the maximum amplitude of the disturbance falls off and the period becomes shorter, which suggests that the low wavenumber disturbances should dominate if instability is present.

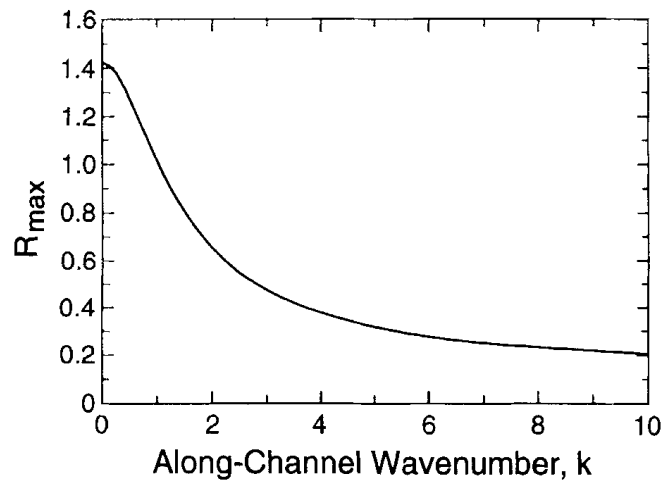


Figure 4 Plot of R_{\max} versus k for $l = 1.0$, [from equation (4.29)].

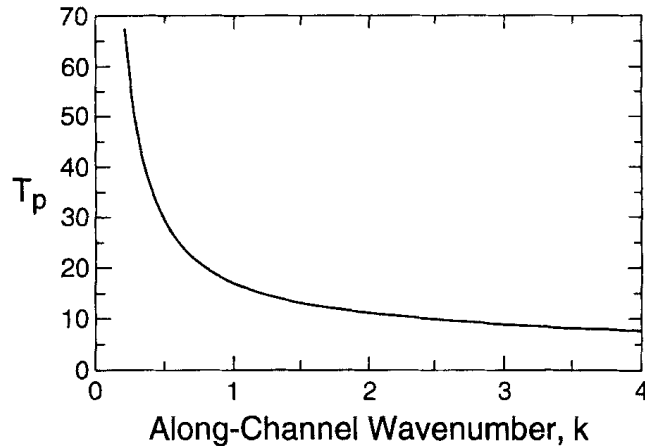


Figure 5 Plot of period versus k for $l = 1.0$, [from equation (4.32)].

5. AMPLITUDE EQUATIONS FOR THE $K = 1$ MODE

5.1. Derivation of the equations

In this section, we examine the nonlinear development of a slightly supercritical $K = 1$ mode, which is the wavenumber modulus corresponding to the mode located at the minimum of the marginal stability curve (see Figure 2) for which $\gamma_c = 0$. Under these conditions, a small but finite positive γ will lead to a narrow band of unstable modes centered on $K = 1$. We wish to follow the evolution of the resulting baroclinic wave packet as it goes initially unstable and interacts with itself.

The evolution of the marginally unstable $K = 1$ mode is singular in the sense that it cannot be described by simply taking the limit $K \rightarrow 1$, $\gamma_c \rightarrow 0$ and $c \rightarrow 1$ of the theory developed in Section 4 for the $K \neq 1$ modes. One immediate difference between the marginally unstable $K = 1$ and $K \neq 1$ modes which has significance follows from (4.8), where we see that the leading order amplitude in the lower layer satisfies $B \rightarrow 0$ in the limit $K \rightarrow 1$. This implies that the leading order term $h^{(0)}(x, y, t; T) \equiv 0$ in the expansion (4.4) for $K \equiv 1$. This is equivalent to observing that, to leading order, the two layers are decoupled for this marginally unstable mode.

However, this point alone is not sufficient to establish that the theory developed in Section 4 will not describe the finite-amplitude evolution of a marginally unstable $K = 1$ mode. Indeed, if one takes the limit $K \rightarrow 1$, $\gamma_c \rightarrow 0$ and $c \rightarrow 1$ of the various coefficients in Section 4, it is easily seen that $\eta^{(0)}$, $\eta^{(1)}$, $h^{(0)}$ and $h^{(1)}$ all remain finite. The problem first arises in equation (4.22) where it is seen that $\eta^{(2)}$ and hence $h^{(2)}$ become singular in this limit. As we will show later in this section, the problem can be traced to the fact that the theory developed for h in Section 4 does not need to include the additional higher harmonics required in this section.

In addition, as we saw in Section 3, the phase speed of the marginally unstable $K = 1$ mode will be given by $c = 1$. This is nothing more than a reflection of the fact that, to leading order, it follows from (3.3b) that the dynamics of the lower layer perturbation height is described by $h_t + h_x = 0$ in the weakly nonlinear marginally unstable limit (recall that we set $U_0 \equiv 0$).

The fact that $c = 1$ means that the entire lower layer is a critical layer. Note that it follows from (2.4) that the leading order Eulerian velocity field in the lower layer is given by $\mathbf{u}_2 \simeq \mathbf{e}_1$. The steady velocity in the lower layer given by $\mathbf{u}_2 \simeq \mathbf{e}_1$, which we have previously (e.g., Swaters and Flierl, 1991) referred to as the Nof velocity, arises due to the geostrophic adjustment of a density-driven flow lying directly on a sloping bottom (see, e.g., Nof, 1983). The phase speed of the marginally unstable $K = 1$ mode is therefore identical everywhere in the lower layer to the induced Nof velocity and the entire lower layer forms a critical layer. As is well known (see, e.g., Benny and Bergeron, 1969, or Warn and Gauthier, 1989), there will be a rapid development of the dimensionality of the underlying phase space as more and more modes are excited by the fundamental harmonic due to the intrinsic nonlinearity of the critical layer.

From the point of view of the asymptotics, the nonlinear development of the marginally unstable $K = 1$ mode will, of course, be determined by the higher order terms in (3.2b). However, since the leading order equation for h is nondispersive, it necessarily follows that all the higher harmonics associated with the nonlinear terms in (3.2b) will generate secular producing terms. These secular producing higher harmonics, which must be removed in a properly constructed asymptotic theory, lead inevitably to an infinity of wave packet evolution equations in sharp contrast to the single mode theory for the $K \neq 1$ modes developed in Section 4.

In order to examine the nonlinear evolution of the marginally unstable $K = 1$ mode it is convenient to move into a co-moving reference frame in which the frequency, to leading order in the lower layer, will be zero. In this reference frame, the time development of the current height will be determined by the higher order, and importantly, the Jacobian, terms in (3.2b). To this end, and in light of the preceding comments, the correct scalings for the perturbation fields for the marginally unstable $K = 1$ mode will be given by

$$\left. \begin{aligned} \eta(x, y, t) &= \varepsilon \tilde{\eta}(\tilde{x}, y; X, T), \\ h(x, y, t) &= \varepsilon^2 \tilde{h}(\tilde{x}, y; X, T), \\ \tilde{x} &= x - t, \quad T = \varepsilon t, \quad X = \varepsilon x, \end{aligned} \right\} \quad (5.1)$$

where the slope of the slightly supercritical gravity current thickness will be given by

$$\gamma = \varepsilon^2, \quad (5.2)$$

where we assume $0 < \varepsilon \ll 1$.

If we substitute (5.1) and (5.2) into (3.2) and (3.6), appreciating that time and space derivatives map according to $\partial_t \mapsto -\partial_{\tilde{x}} + \varepsilon \partial_T$ and $\partial_x \mapsto \partial_{\tilde{x}} + \varepsilon \partial_X$, respectively, we get,

after dropping the tildes

$$(\nabla^2 + 1)\eta_x = \varepsilon [\nabla^2 \eta_T - 2\eta_{x_{xx}} - \eta_x - h_x + J(\eta, \nabla^2 \eta)] + O(\varepsilon^2), \quad (5.3)$$

$$h_T + h_x - \eta_x + J(\eta, h) = 0 + O(\varepsilon). \quad (5.4)$$

The solution to (5.3) and (5.4) is constructed via the straightforward asymptotic expansion

$$\left. \begin{aligned} \eta(x, y; X, T) &= \eta^{(0)}(x, y; X, T) + \varepsilon \eta^{(1)}(x, y; X, T) + \dots, \\ \eta(x, y; X, T) &= \eta^{(0)}(x, y; X, T) + \varepsilon \eta^{(1)}(x, y; X, T) + \dots, \end{aligned} \right\} \quad (5.1)$$

Substituting (5.5) into (5.3) and (5.4) leads to the $O(1)$ problem

$$(\nabla^2 + 1)\eta_x^{(0)} = 0, \quad (5.6)$$

$$h_T^{(0)} + h_x^{(0)} - \eta_x^{(0)} + J(\eta^{(0)}, h^{(0)}) = 0. \quad (5.7)$$

The solution to (5.6) is written in the form

$$\eta^{(0)}(x, y; X, T) = A(X, T) \sin(l y) \exp(ikx) + \text{c.c.}, \quad (5.8)$$

where $l = \xi/L$ and $k^2 + l^2 \equiv K^2 = 1$ and where $A(X, T)$ is, at this stage, an arbitrary slowly-varying amplitude function.

To determine $A(X, T)$ and close the system of equations we must examine the $O(\varepsilon)$ problem associated with the upper layer, which is given by

$$(\nabla^2 + 1)\eta_T^{(1)} = \nabla^2 \eta_x^{(0)} - 2\eta_{x_{xx}}^{(0)} - \eta_x^{(0)} - h_x^{(0)}, \quad (5.9)$$

where we have used $J(\eta^{(0)}, \nabla^2 \eta^{(0)}) \equiv 0$ which follows from (5.6) and (5.8).

The terms on the right-hand side of (5.9) which will produce secular growth are those terms which are proportional to $\sin(l y) \exp(ikx)$ and its complex conjugate. We may therefore write the solvability condition associated with (5.9) in the form

$$\int_0^L \int_0^{2\pi/k} [\nabla^2 \eta_T^{(0)} - 2\eta_{x_{xx}}^{(0)} - \eta_x^{(0)} - h_x^{(0)}] \sin(l y) \exp(-ikx) dx dy = 0, \quad (5.10)$$

where the complex conjugate of this relationship is understood. Equation (5.10) is simply the geometric statement that the projection of the right-hand side of (5.9) on the $\sin(l y) \exp(\pm ikx)$ mode must be zero.

Equations (5.7) and (5.10) form a closed system of partial differential equations for $h^{(0)}(x, y; X, T)$ and $A(X, T)$. We have chosen to write the coupled equations in this

way in order to emphasize the similarity with the analysis presented by Warn and Gauthier (1989) for a marginally unstable baroclinic flow in the Philip's model. We point out that if one neglects the ∂_x derivatives in (5.7) and (5.10), it is possible to obtain a closed form solution to (5.7) and (5.10) in terms of elliptic and trigonometric functions by a slight modification of the methods presented in Warn and Gauthier (1989). We have not been able to generalize the Warn and Gauthier technique to the equations if one retains slow space variations in the wave amplitudes and thus we construct a solution using the spectral approach developed by Pedlosky (1982a) for wave packets in a marginally unstable baroclinic flow in the Phillip's model.

Before we construct the spectral solution to (5.7) and (5.10) it is useful to describe the qualitative difference between (5.7) and (5.10) and (4.23). Equations (5.8) and (5.10) suggest writing the solution for $h^{(0)}(x, y, X, T)$ in the form

$$h^{(0)}(x, y, X, T) = i/k[\partial_T + (1 - 2k^2)\partial_X]A(X, T)\exp(ikx)\sin(l y) + \text{c.c.} \\ + \phi(y, X, T) + \psi(x, y, X, T), \tag{5.11}$$

where $\phi(y, X, T)$ and $\psi(x, y, X, T)$ are the real-valued x -independent contribution, i.e., the mean flow contribution, and higher along-channel and cross-channel harmonics, respectively, i.e.,

$$\left. \begin{aligned} \phi(y, X, T) &= \frac{k}{2\pi} \int_0^{2\pi/k} h^{(0)}(x, y, X, T) dx, \\ \int_0^{2\pi/k} \psi(x, y, X, T) dx &= 0, \\ \int_0^{2\pi/k} \sin(l y) \exp(\pm ikx) \psi(x, y, X, T) dx &= 0. \end{aligned} \right\} \tag{5.12}$$

Substitution of (5.11) into (5.7) leads to the system of equations

$$\{(\partial_T + \partial_X)[\partial_T + (1 - 2k^2)\partial_X] - k^2\}A + \frac{2lk^2 A}{\pi} \int_0^{\pi/l} \sin^2(l y) \phi_y dy = 0, \tag{5.13}$$

$$(\partial_T + \partial_X)\phi + l \sin(2ly)[\partial_T + (1 - 2k^2)\partial_X]|A|^2 \\ + \frac{k}{2\pi} \int_0^{2\pi/k} J[A \sin(l y) \exp(ikx) + \text{c.c.}, \psi] dx = 0, \tag{5.14}$$

$$(\partial_T + \partial_X)\psi + J[A \sin(l y) \exp(ikx) + \text{c.c.}, \psi] \\ - \frac{k}{2\pi} \int_0^{2\pi/k} J[A \sin(l y) \exp(ikx) + \text{c.c.}, \psi] dx = \\ \frac{1}{4} l \exp(2ikx) \sin(2ly) [\partial_T + (1 - 2k^2)\partial_X]A^2 + \text{c.c.} \tag{5.15}$$

The most important difference between (5.13), (5.14) and (5.15) compared with (4.23) is the presence of the higher harmonic $\exp(\pm 2ikx)\sin(2ly)$ term on the right-hand-side of (5.15). There is no analogue of this term in (4.23). Observe that if there was no “forcing” of this sort in (5.15), it would follow that we could choose $\psi = 0$ as a solution to (5.15). In turn, it is easy to verify that setting $\psi = 0$ in (5.14) and eliminating ϕ from between (5.13) and (5.14) leads to (4.23) assuming $K = 1$ and ignoring the slow spatial derivatives. The higher harmonics associated with the nonlinear $J(\eta^{(0)}, h^{(0)})$ term in (5.7) play a crucial role in describing the finite-amplitude evolution of a marginally unstable $K = 1$ mode.

5.2. Spectral solution for $h^{(0)}(x, y, X, T)$

Here we construct an explicit spectral solution for $h^{(0)}$ in the form

$$h^{(0)} = \phi(y, X, T) + \left\{ \sum_{m=1}^{\infty} \sum_{n=1}^{\infty} B_{m,n}(X, T) \sin(nly) \exp(mikx) + \text{c.c.} \right\}. \quad (5.16)$$

The $B_{1,1}(X, T)$ term in (5.16) will, of course, be given by $ik^{-1}[\partial_T + (1 - 2k^2)\partial_X]A(X, T)$ as suggested by (5.11). This will be shown momentarily.

We remark that the phase velocities for the upper and lower layers are the same, but the group velocities will be different, viz

$$c_{g1} = \frac{d}{dk} \left[\frac{k}{k^2 + l^2} \right] = 1 - 2k^2, \quad (5.17)$$

(since $k^2 + l^2 = 1$) and

$$c_{g2} = 1. \quad (5.18)$$

where the subscripts 1 and 2 denote the upper and lower layer respectively. The phase velocities ‘coalesce’ at the $K = 1$ mode, but the group velocities remain distinct. This is exactly the same observation made by Pedlosky (1972; 1982a) for the Phillip’s model.

Substituting (5.16) into (5.10) leads to

$$ikB_{1,1} + A_T + (1 - 2k^2)A_X = 0. \quad (5.19)$$

This equation determines $B_{1,1}(X, T)$ as a function of $A(X, T)$.

Substituting (5.8) and (5.16) into (5.7) yields

$$\begin{aligned}
 & ikA(1 - \phi_y)\sin(ly)\exp(ikx) \\
 & - \frac{1}{2}iklA \sum_{m=1}^{\infty} \sum_{n=1}^{\infty} \{nB_{m,n}\sin[(n+1)ly] - (n+1)B_{m,n+1}\sin(nly) \\
 & - mB_{m,n}\sin[(n+1)ly] - mB_{m,n+1}\sin(nly)\}\exp[(m+1)ikx] \\
 & + \frac{1}{2}iklA^* \sum_{m=1}^{\infty} \sum_{n=1}^{\infty} \{nB_{m,n}\sin[(n+1)ly] - (n+1)B_{m,n+1}\sin(nly) \\
 & + mB_{m,n}\sin[(n+1)ly] + mB_{m,n+1}\sin(nly)\}\exp[(m-1)ikx] \\
 & - \sum_{m=1}^{\infty} \sum_{n=1}^{\infty} (B_{m,nX} + B_{m,nT})\sin(nly)\exp(mikx) + \text{c.c.} - \phi_X - \phi_T = 0. \quad (5.20)
 \end{aligned}$$

This expression is a double Fourier series in the orthogonal basis functions $\{\sin(nly)\}_{n=1}^{\infty}$ and $\{\exp(mikx)\}_{m=0}^{\infty}$. The evolution equations are obtained by demanding that each individual Fourier coefficient be identically zero.

The terms which are independent of the fast phase x are given by

$$\begin{aligned}
 \phi_X + \phi_T = \frac{1}{2}iklA^* \sum_{n=1}^{\infty} \{nB_{1,n}\sin[(n+1)ly] - (n+1)B_{1,n+1}\sin(nly) \\
 + B_{1,n}\sin[(n+1)ly] + B_{1,n+1}\sin(nly)\} + \text{c.c.} \quad (5.21)
 \end{aligned}$$

Simplifying and including the complex conjugate explicitly, we find that

$$\begin{aligned}
 \phi_X + \phi_T = \frac{1}{2}ikl \sum_{n=1}^{\infty} \{n(AB_{1,n+1}^* - A^*B_{1,n+1}) \\
 - n(AB_{1,n-1}^* - A^*B_{1,n-1})\} \sin(nly). \quad (5.22)
 \end{aligned}$$

The solution to (5.22) may be written in the form

$$\phi = \frac{1}{2}l \sum_{n=1}^{\infty} \alpha_n(X, T)n\sin(nly). \quad (5.23)$$

Substituting (5.23) into (5.22) leads to the following set of equations for α_n

$$\alpha_{nX} + \alpha_{nT} = ik[(AB_{1,n+1}^* - A^*B_{1,n+1}) - (AB_{1,n-1}^* - A^*B_{1,n-1})]. \quad (5.24)$$

We shall now examine the $\exp(ikx)$ terms. Extracting from (5.20) all terms of this form yields

$$\begin{aligned}
 & ikA(1 - \phi_y)\sin(ly) + \frac{1}{2}iklA^* \sum_{n=1}^{\infty} \{nB_{2,n}\sin[(n+1)ly] \\
 & - (n+1)B_{2,n+1}\sin(nly) + 2B_{2,n}\sin[(n+1)ly] + 2B_{2,n+1}\sin(nly)\} \\
 & - \sum_{n=1}^{\infty} (B_{1,nX} + B_{1,nT})\sin(nly) = 0. \tag{5.25}
 \end{aligned}$$

If (5.23) is substituted into (5.25), we find, after some manipulation

$$ikA + l^2 ikA\alpha_2 - B_{1,1X} - B_{1,1T} = 0, \tag{5.26}$$

from the $\sin(ly)$ terms, and from the $\sin(nly)$ terms ($n > 1$),

$$\begin{aligned}
 & -\frac{1}{4}l^2 kA [(n-1)^2 \alpha_{n-1} - (n+1)^2 \alpha_{n+1}] \\
 & + \frac{1}{2}iklA^* [(n+1)B_{2,n-1} - (n-1)B_{2,n+1}] \\
 & - (B_{1,nX} + B_{1,nT}) = 0, \quad (n = 2, 3, \dots). \tag{5.27}
 \end{aligned}$$

And finally, the equations associated with the modes where $m > 1$ are found in exactly an analogous way, and are given by

$$\begin{aligned}
 B_{m,nT} + B_{m,nX} &= \frac{1}{2}iklA^* [(n+m)B_{m+1,n-1} - (n-m)B_{m+1,n+1}] \\
 & - \frac{1}{2}iklA [(n-m)B_{m-1,n-1} - (n+m)B_{m-1,n+1}], \tag{5.28}
 \end{aligned}$$

for $m = 2, 3, \dots$, and $n = 1, 2, \dots$

Equation (5.28) can be consolidated with (5.27) to yield equations for all $B_{m,n}$ and if (5.19) is substituted into (5.26) to generate an equation for α_2 , then a complete, closed, infinite set of nonlinear partial differential equations is the result. To simplify these resulting equations, we introduce the transformations

$$\left. \begin{aligned}
 \alpha_n &= -\tilde{\alpha}_n, \\
 B_{m,n} &= -i\tilde{B}_{m,n}, \text{ (except for } B_{1,1}\text{),}
 \end{aligned} \right\} \tag{5.29}$$

which yields the coupled system (after dropping the tildes)

$$(\partial_T + \partial_X) [\partial_T + (1 - 2k^2) \partial_X] A = k^2 A - l^2 k^2 A \alpha_2, \quad (5.30)$$

$$(\partial_T + \partial_X) \alpha_2 = [\partial_T + (1 - 2k^2) \partial_X] |A|^2 + k(AB_{1,3}^* + A^*B_{1,3}), \quad (5.31)$$

$$(\partial_T + \partial_X) \alpha_n = k [(AB_{1,n+1}^* + A^*B_{1,n+1}) - (AB_{1,n-1}^* + A^*B_{1,n-1})], \quad (5.32)$$

for $n = 1, 3, 4, \dots$, and

$$\begin{aligned} (\partial_T + \partial_X) B_{m,n} = & -\frac{1}{4} l^2 k A [(n-1)^2 \alpha_{n-1} - (n+1)^2 \alpha_{n+1}] \delta_{1,m} \\ & + \frac{1}{2} iklA^* [(n+m) B_{m+1, n-1} - (n-m) B_{m+1, n+1}] \\ & - \frac{1}{2} iklA [(n-m) B_{m-1, n-1} - (n+m) B_{m-1, n+1}] \end{aligned} \quad (5.33)$$

for $m = 1, 2, \dots, n = 1, 2, 3, \dots$ (except $m = n = 1$).

Equations (5.30) through to (5.33) define the evolution in slow time and space of the perturbation pressure amplitude $A(X, T)$, all the modes of the gravity current height $B_{m,n}(X, T)$, and all the mean flow modes $\alpha_n(X, T)$. It is important to note that each mode does not interact directly with all the others; a mode interacts only with a small band of its nearest 'neighbors'. This makes the system more tractable numerically, especially if ∂_X or ∂_T is set to zero. The major problem here is the determination of an appropriate point to truncate the system so as to work with a closed, finite set of equations, but at the same retain as much of the physics that the infinite system represents as possible.

There is an interesting point to notice about the equations (5.30) through to (5.33) before any analysis is done. It can immediately be seen that the 'ladder' of excited modes is initiated by the presence of the $B_{1,3}$ amplitude coefficient in (5.33). This 'odd' mode excites only 'even' mean flow modes (i.e. α_{2n}) and only 'even-even' or 'odd-odd' pairs of height perturbation modes (i.e. $B_{2,3}, B_{2,5}$ etc. = 0). So although the excluded coefficients are represented in the equations, they are not forced by the perturbation pressure.

5.3. Solutions to the equation set

5.3.1. Solitary eddy solution

It is possible to derive a steadily-travelling solution to a truncated set of the equations (5.30) through to (5.33). If we retain only (5.30) and (5.31) and neglect $B_{1,3}$ and

higher order terms, we are left with the coupled set of equations

$$(\partial_T + \partial_X)[\partial_T + (1 - 2k^2)\partial_X]A = k^2A - k^2l^2A\alpha_2, \quad (5.34)$$

$$(\partial_T + \partial_X)\alpha_2 = [\partial_T + (1 - 2k^2)\partial_X]|A|^2. \quad (5.35)$$

These equations correspond to retaining only the fundamental harmonic and its accompanying mean flow, and are identical in form to those derived by Pedlosky (1972) in his original (incorrect) marginally unstable wave packet analysis of the Phillip's model of baroclinic instability.

It is straightforward to verify that there exists a steadily-travelling solution to these truncated equations of the form

$$A(X, T) = A(\xi), \quad \alpha_2(X, T) = \alpha_2(\xi). \quad (5.36)$$

where $\xi = X - VT$. Substituting (5.36) into (5.34) and (5.35) leads to the solution

$$A(\xi) = A_0 \operatorname{sech}(\kappa\xi), \quad \alpha_2(\xi) = \left(\frac{1 - 2k^2 - V}{1 - V} \right) A_0 \operatorname{sech}^2(\kappa\xi), \quad (5.37, 38)$$

where A_0 is the maximum envelope amplitude, and where

$$V = \frac{2k^2 - A_0^2 l^2 k^2 (1 - 2k^2)}{2k^2 - A_0^2 l^2 k^2}, \quad (5.39)$$

$$\kappa = \left(\frac{A_0^2 l^2 k^2}{2} \right)^{1/2} \frac{2k^2 - A_0^2 l^2 k^2}{2A_0^2 l^2 k^4}. \quad (5.40)$$

We may determine the perturbation thickness amplitude from (5.19) which yields

$$B_{1,1}(\xi) = i \left[\frac{A_0 \kappa (V - 1 + 2k^2)}{\kappa} \right] \operatorname{sech}(\kappa\xi) \tanh(\kappa\xi). \quad (5.41)$$

We now follow a similar procedure to that employed in Subsection 4.2 and analyze this solution in the context of a channel. Here we let $k = 0.5$, which implies $l \approx 0.866$ so that $k^2 + l^2 = 1$. This implies a dimensional channel width of about 54 km, and that $V \approx 1.052$ and $\kappa \approx 2.960$. Figure 6a is a contour plot for the upper layer perturbation pressure

$$\eta_0(x, y, 0, X, 0) = 2A_0 \operatorname{sech}(\kappa X) \cos(\kappa x) \sin(l y), \quad (5.42)$$

assuming an initial non-dimensional amplitude of $A_0 = 0.5$, assuming time is fixed (i.e. a 'snapshot' in time), and with $\varepsilon = 0.1$. The figure shows clearly that for these parameter values the solitary wave is approximately the size of three pressure cells, and so at any one time three cells or parts of four cells are visible as the wave

propagates along the channel. Since V , the speed of the solitary wave, is larger than the phase speed c the fast oscillations will appear in front of the wave, reach their apex at the maximum amplitude of the solitary wave, and disappear again behind the moving wavepacket.

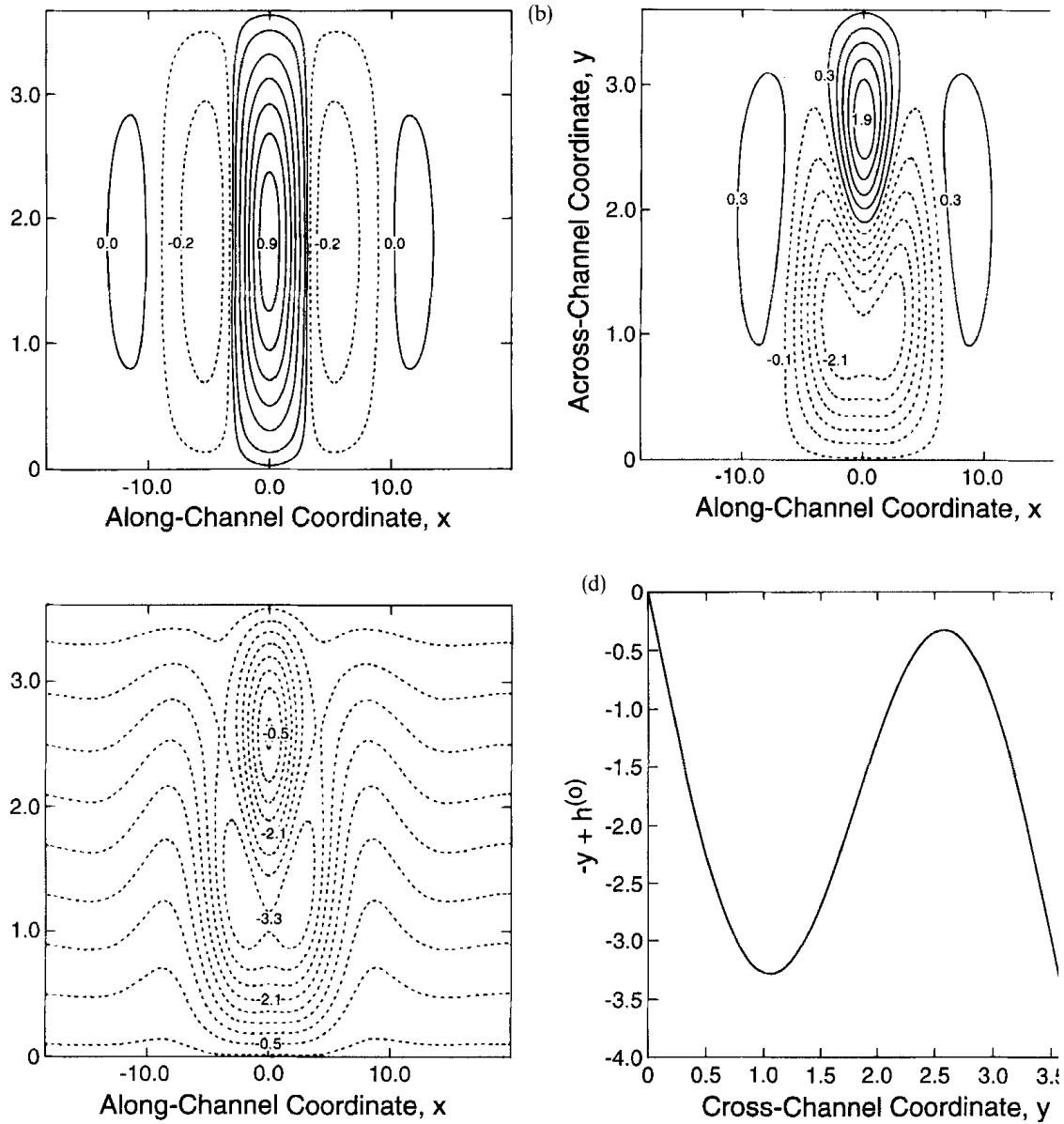


Figure 6a, b, c, d Contour plots of leading order non-dimensional perturbation (a) pressure (b) thickness and (c) leading order variable part of the total current height scaled by ε^{-2} where $k = 0.5$, $l = 0.866$, and $A_0 = 0.5$. The contour intervals in (a), (b) and (c) are approximately ± 0.15 , ± 0.4 and ± 0.4 , respectively. Figure 6d depicts a section along $x = 0.0$ from Figure 6c. Note the distinct positive anomaly centered at approximately $y \approx 2.5$.

A plot of the gravity current thickness perturbation

$$h_0(x, y, 0, X, 0) = -l \frac{(1 - 2k^2 - V)}{(1 - V)} A_0^2 \operatorname{sech}^2(\kappa X) \sin(2ly) + 2A_0 \kappa \frac{(V - 1 + 2\kappa^2)}{\kappa} \operatorname{sech}(\kappa X) \tanh(\kappa x + \pi/2) \sin(ly), \quad (5.43)$$

using the same data as above is shown in Figure 6b. We see that the mean flow adjustment dominates and that the plane wave component simply distorts these cross-channel high and low thickness cells. Figure 6c is a plot of the $O(\varepsilon^2)$ contribution to the total current height, i.e., the leading order nonconstant part of the total current height given by $[(3.6) + \varepsilon^2(5.38) - h_{\text{MAX}}]/\varepsilon^2$ where it is understood that $\gamma = \varepsilon^2$. Note that there is a distinct positive thickness anomaly centered at approximately $(x, y) \simeq (0.0, 2.5)$. This positive thickness anomaly is depicted in Figure 6d, which corresponds to a section along $x = 0.0$ in Figure 6c. This anomaly represents a steadily travelling cold dome, and so this solution strongly suggests the possibility that instabilities in the model could evolve into isolated cold domes.

We note however that there is some question regarding the stability of this solitary wave solution over time. Gibbon *et al.* (1979) have shown that (5.34) and (5.35) may be combined into a sine-Gordon equation. They concluded that if the linear growth rate is positive, then the disturbance is itself unstable to small perturbances on the ‘tail’ of the wave because there is a source of available potential energy there. We have not been able to determine the role of the higher harmonics in the evolution of this solution, or if similar solutions exist for higher order truncations.

5.3.2. Higher order truncations

All of our remaining analysis will be done by setting $\partial_x = 0$ in the system (5.30) through to (5.33). With this assumption made, some points of interest should be noted here. First, if $B_{1,3}$ is set to zero in (5.31) and the equation is then integrated with respect to the slow time T , we find that

$$\alpha_2(T) = |A(T)|^2 - |A(0)|^2. \quad (5.44)$$

If this equation is substituted into (5.30), we find that the result is equivalent to (4.23) if we apply it to the most unstable mode (i.e. set $k^2 + l^2 = 1$ in that equation). Another interesting aspect here is that if we sum all equations represented by (5.32) and add them to (5.31), we find the following

$$\sum_{n=1}^{\infty} \frac{d\alpha_{2n}}{dT} = \frac{d|A|^2}{dT}, \quad (5.45)$$

which leads immediately to

$$\sum_{n=1}^{\infty} \alpha_{2n} = |A|^2 - |A_0|^2. \tag{5.46}$$

Equation (5.41) implies that, if all the excited modes are represented, that the sum of all the mean flow adjustment amplitudes at any time T is equal to the modulus squared of the free surface perturbation amplitude to within a constant. This suggests strongly that, if the assumption is made that A is bounded, the mean flow modes fall off in importance as the ‘ladder’ is climbed, but there is no proof for this (because we cannot claim that $\alpha_{n+2} < \alpha_n$ for all n).

We now examine in more detail system of equations (5.30) through to (5.33). Two different truncation points are applied, and standard Runge-Kutta methods are used to integrate the resulting set of equations numerically. We first derive a simple system of four equations, where two mean flow modes are included as follows

$$\left. \begin{aligned} \frac{d^2 A}{dT^2} &= k^2 A - l^2 k^2 A \alpha_2, \\ \frac{d\alpha_2}{dT} &= \frac{d|A|^2}{dT} + k(AB_{1,3}^* + A^*B_{1,3}), \\ \frac{dB_{1,3}}{dT} &= -\frac{l^2 k A}{4} (4\alpha_2 - 16\alpha_4), \\ \frac{d\alpha_4}{dT} &= -k(AB_{1,3}^* + A^*B_{1,3}). \end{aligned} \right\} \tag{5.47}$$

In order to simplify the system (5.47), we assume that all variables have constant phases, which allows us to use the linear theory growth rate as an initial condition (as mentioned in Subsection 4.1) on the perturbation pressure amplitude. We use the same parameter settings as in the previous subsection, except here we set the non-dimensional initial amplitude $A_0 = 0.01$. Standard Runge-Kutta methods for solving systems of Odes were then applied, and the results for A and $\text{Im}[B_{1,1}]$ are plotted on Figure 7a and 7b, respectively. The non-dimensional perturbation pressure amplitude reaches about two orders of magnitude greater than the initial perturbation amplitude before nonlinear effects finally halt the growth. The timescale of the disturbance is again very long, similar to what was found in Section 4, and it is again due to the very small supercriticality applied to the gravity current thickness.

In Figures 8a and 8b, we plot A and $\text{Im}[B_{1,1}]$, respectively, for a system of 12 equations, which essentially amounts to adding one more mean flow mode (α_6) and including perturbation thickness modes upto $B_{2,4}$ and $B_{3,5}$ to make a complete set (to work with real valued functions only, we set $\tilde{B}_{2m,2n} = -i\hat{B}_{2m,2n}$). The figure shows a very similar result, where the pressure amplitude again grows to approximately 180 times the initial amplitude before nonlinearities stop and reverse the growth. It is interesting to note that the amplitude oscillates as before, but several more cycles are required to form a period than in the 4 equation system.

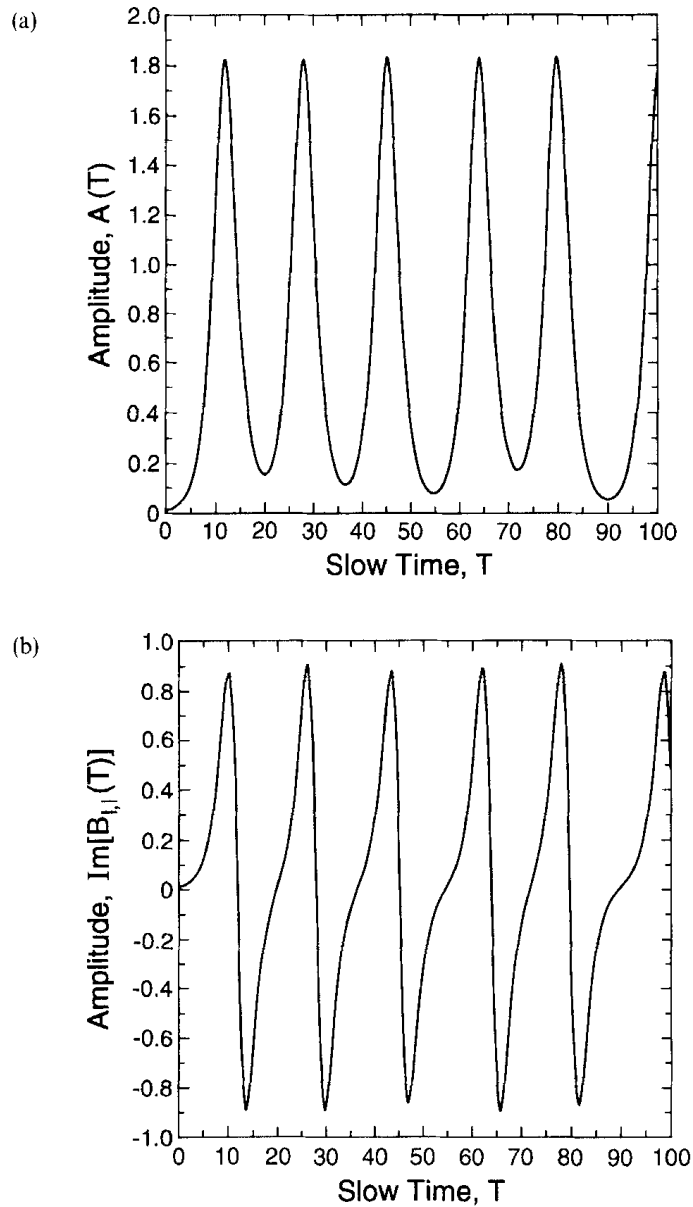


Figure 7a,b Plot of temporal solution for (a) $A(T)$ and (b) $\text{Im}[B_{1,1}(T)]$ for the 4 equation set (5.38) where $k = 0.5$, $l = 0.866$, and $A_0 = 0.01$.

Other truncations were applied [not presented here, see Mooney (1995)] and it was found, in general, that if the cutoff was applied too soon after (but not directly after) a mean flow mode, then exponentially growing solutions resulted for $A(T)$. If the truncations was applied directly after a mean flow mode, then the equation set yielded bounded oscillating solutions, where the cycles forming a period became more complex with each increase in size of the set. This would seem to indicate that

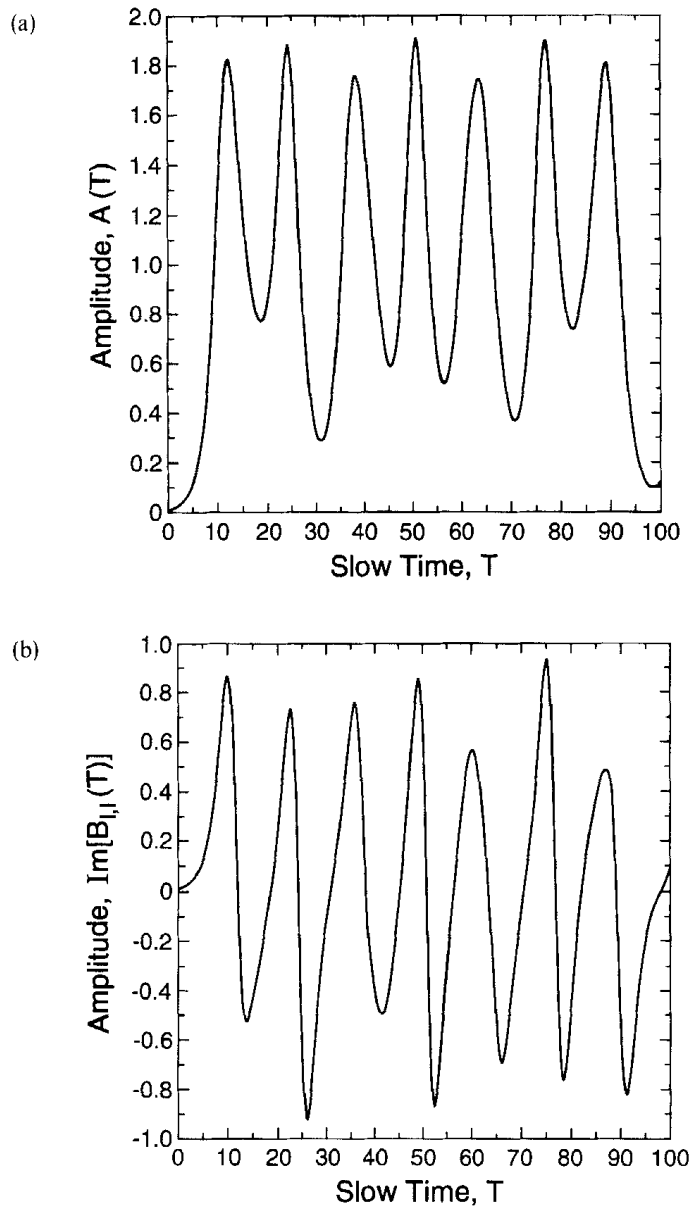


Figure 8a, b Plot of temporal solution for (a) $A(T)$ and (b) $\text{Im}[B_{1,1}(T)]$ for the 12 equation set truncated at α_6 , $B_{2,4}$ for even gravity current modes and $B_{3,5}$ for odd gravity current modes. Parameters are the same as in Figures 7a, b.

the mean flow modes have a stabilizing influence on the solutions, possibly by acting to restrict the potential energy available to the higher modes. We were unable to rigorously establish whether or not increasing the number of modes always leads to an increase in the number of cycles needed to form a period, although the numerical evidence seems to indicate this.

6. SUMMARY AND CONCLUSIONS

In this paper, a theory has been developed to describe the weakly nonlinear stability characteristics of a baroclinic mesoscale gravity current in a channel with a sloping bottom. The model assumes that the gravity current evolves geostrophically but not quasi-geostrophically, because the interface deflections are not small compared to the scale depth of the current. The ambient channel water dynamics are quasi-geostrophic, however, which leads to strong interaction between the geostrophic pressure and the height of the front.

Linear stability theory was applied to the model in order to generate a marginal stability curve which relates the rate of change of gravity current thickness to the horizontal wavenumber. We then utilized weakly nonlinear stability theory to derive finite-amplitude equations which follow the evolution of unstable mode after application of a small supercriticality to the gravity current thickness slope. It was found that if the wavenumber was not at the bottom of the marginal stability curve, then the amplitude of the wave is periodic in time and it takes the form of a Jacobi dnoidal function.

If the supercriticality is centered on the mode at the bottom of the marginal stability curve, then an infinite set of nonlinear partial differential equations, in slow space and time, are required to describe the finite-amplitude evolution of the flow. These equations link the perturbation pressure amplitude to an infinite number of modes for the amplitude of the frontal thickness and the mean flow adjustment. If the truncation of this set is applied so that only the perturbation pressure and the first mode for the mean flow adjustment are included, then solitary wave solutions are possible, similar to those generated by Pedlosky (1972). If more modes are included then numerical integrations of the spatially-independent equations suggest that the solutions are oscillatory.

The theory shows that the retention of the nonlinear interaction terms in the stability equations sets up a balance between the tendency of the wave to extract potential energy and grow, and the adjustment to the mean flow which necessarily results from this, which reduces the available potential energy and so shows the growth. This balance produces an oscillation between states of maximum amplitude and minimum available potential energy, and vice versa. The 'saturation' and eventual reversal of the initially exponential growth rate of the disturbance makes it possible to think of this as a mechanism for the breakup of the gravity current into coherent cold eddies.

Acknowledgments

Support for the preparation of this paper was provided in part by a research Grant awarded by the Natural Sciences and Engineering Research Council of Canada and a Science Subvention awarded by the Department of Fisheries and Oceans of Canada to G.E.S, and a Province of Alberta Graduate Scholarship awarded to C.J.M. We wish to thank T.G. Shepherd for pointing out the existence of the paper by Warn and Gauthier and to the Referees for making several valuable suggestions which substantially improved the paper.

References

- Armi, L. and D'Asaro, E., "Flow structures in the benthic ocean," *J. Geophys. Res.* **85**, 469–483 (1980).
- Benney, D. J. and Bergeron, R. F., "A new class of nonlinear waves in parallel flows," *Stud. Appl. Math.* **48**, 181–204 (1969).
- Gibbon, J. D., James, I. N. and Moroz, I. M., "An example of soliton behavior in a rotating baroclinic fluid," *Proc. R. Soc. Lond.* **A367**, 219–237 (1979).
- Griffiths, R. W., Killworth, P.D. and Stern, M.E., "Ageostrophic instability of ocean currents," *J. Fluid Mech.* **117**, 343–377 (1982).
- Houghton, R. W., Schlitz, R., Beardsley, R. C., Butman, B. and Chamberlin, J. C., "The middle Atlantic bight pool: evolution of the temperature structure during 1979," *J. Phys. Oceanogr.* **12**, 1019–1029 (1982).
- Karsten, R. H., Swaters, G. E. and Thomson, R. E., "Stability characteristics of deep-water replacement in the Strait of Georgia," *J. Phys. Oceanogr.* **25**, 2391–2403 (1995).
- Leblond, P. H. and Mysak, L. A., *Waves in the Ocean*, Elsevier (1978).
- LeBlond, P. H., Ma, H., Doherty, F. and Pond, S., "Deep and intermediate water replacement in the Strait of Georgia," *Atmosphere-Ocean* **29**, 288–312 (1991).
- Milne-Thomson, L. M., *Jacobian Elliptic Function Tables*, Dover (1950).
- Mooney, C. J., "Finite amplitude baroclinic instability of a mesoscale gravity current in a channel," M.Sc. Thesis, University of Alberta, Edmonton, Canada (1995).
- Mory, M., Stern, M.E and Griffiths, R. W., "Coherent baroclinic eddies on a sloping bottom," *J. Fluid Mech.* **183**, 45–62 (1987).
- Nof, D., "The translation of isolated cold eddies on a sloping bottom," *Deep Sea Res.* **30**, 171–182 (1983).
- Paldor, N. and Killworth, P.D., "Instabilities of a two-layer coupled front," *Deep Sea Res.* **34**, 1525–1539 (1987).
- Pedlosky, J., "Finite amplitude baroclinic waves," *J. Atmos. Sci.* **27**, 15–30 (1970).
- Pedlosky, J., "Finite amplitude baroclinic wave packets," *J. Atmos. Sci.* **29**, 680–686 (1972).
- Pedlosky, J., "Finite amplitude baroclinic waves at minimum shear," *J. Atmos. Sci.* **39**, 555–562 (1982a).
- Pedlosky, J., "A simple model for nonlinear critical layers in an unstable baroclinic wave," *J. Atmos. Sci.* **39**, 2119–2127 (1982b).
- Pedlosky, J., *Geophysical Fluid Dynamics*, 2nd Edition, Springer (1987).
- Smith, P. C., "Baroclinic instability in the Denmark Strait overflow," *J. Phys. Oceanogr.* **6**, 355–371 (1976).
- Stacey, M. W., Pond, S. and LeBlond, P. H., "An objective analysis of the low frequency currents in the Strait of Georgia," *Atmos.-Ocean* **26**, 1–15 (1988).
- Stacey, M. W., Pond, S. and LeBlond, P. H., "Flow dynamics in the Strait of Georgia, British Columbia," *Atmos.-Ocean* **29**, 1–13 (1991).
- Stacey, M. W., Pond, S., LeBlond, P.H., Freeland, H.J. and Farmer, D.M., "An analysis of the low-frequency current fluctuations in the Strait of Georgia, from June 1984 until January, 1985," *J. Phys. Oceanogr.* **17**, 326–342 (1987).
- Swaters, G. E., "On the baroclinic instability of cold-core coupled density fronts on a sloping continental shelf," *J. Fluid Mech.* **224**, 361–382 (1991).
- Swaters, G. E., "Nonlinear stability of intermediate baroclinic flow on a sloping bottom," *Proc. R. Soc. Lond. A* **442**, 249–272 (1993).
- Swaters, G. E., and Flierl, G. R., "Dynamics of ventilated coherent cold eddies on a sloping bottom", *J. Fluid Mech.* **223**, 565–587 (1991).
- Tan, B. and Liu, S., "Collision interactions of solitons in a baroclinic atmosphere," *J. Atmos. Sci.* **52**, 1501–1512 (1995).
- Warn, T. and Gauthier, P., "Potential vorticity mixing by marginally unstable waves at minimum shear", *Tellus* **41A**, 115–131 (1989).
- Whitehead, J. A. and Worthington, L. U., "The flux and mixing rates of Antarctic Bottom Water within the North Atlantic," *J. Geophys. Res.* **87**, 7903–7924 (1982).
- Zoccolotti, L. and Salusti, E., "Observations on a very dense marine water in the Southern Adriatic Sea," *Continental Shelf Res.* **7**, 535–551 (1987).